Bull. Mater. Sci., Vol. 37, No. 4, June 2014, pp. 883–888. © Indian Academy of Sciences.

Structural, spectroscopic and electrochemical study of V^{5+} substituted $LiTi_2(PO_4)_3$ solid electrolyte for lithium-ion batteries

A VENKATESWARA RAO*, V VEERAIAH, A V PRASADA RAO†, B KISHORE BABU††, B SWARNA LATHA and K RAMA RAO

Department of Physics, †Department of Inorganic and Analytical Chemistry,
††Department of Engineering Chemistry; Andhra University, Visakhapatnam 530 003, India

MS received 30 April 2013; revised 23 September 2013

Abstract. Vanadium substituted $LiTi_2(PO_4)_3$ (LTP) samples of composition of $Li_{1-x}[Ti_{2-x}V_x](PO_4)_3$ (x = 0·0, 0·05, 0·10 and 0·15) have been prepared by solid-state reaction method. XRD data for these compositions indicated the formation of phase pure materials of rhombohedral structure with space group $R\bar{3}c$ (167). Microstructural studies by scanning electron microscope indicated particle size in the range of 0·5–1 μm. Electrochemical impedance studies showed that ionic conductivity is high for x = 0·10 composition. a.c. and d.c. conductivity results up to 573 K are in accordance with the Jonscher's power law. Cyclic voltammetry study showed its electrochemical stability in the voltage range from 0·5 to 3·5 V.

Keywords. Nasicon materials; X-ray diffraction; lithium titanium phosphate; vanadium doped $LiTi_2(PO_4)_3$.

1. Introduction

Many researchers are concentrating on finding high energy density and long life solid-state lithium-ion batteries using solid electrolytes (Birke *et al* 1999; Dhivya *et al* 2013) to power several portable electronic devices such as cell phones, laptops, digital cameras, etc (Bruce *et al* 2008; Ellis *et al* 2010; Goodenough and Kim 2010). Since no other cations except H^+ can penetrate easily into solids than Li^+, the study of rechargeable Li batteries has been actively pursued since 1970s with lithium insertion electrodes (Hong 1976; Aono *et al* 1990; Kasturi Rangan and Gopalakrishnan 1994) in the form of layered $LiCoO_2$ and spinel type $LiMn_2O_4$. On the other hand, NASICON [Na_3Zr_2 $(SiO_4)_2(PO_4)$] structured materials have been explored because of their high ionic conductivity, low thermal expansion coefficient and low thermal conductivity (Goodenough *et al* 1976). NASICON-type materials (isostructural with $NaZr_2(PO_4)_3$) are good ionic conductors with negligible electronic conductivity and they are stable in air (Kosova *et al* 2008). $LiTi_2(PO_4)_3$ (LTP) (Xia and Luo 2009) is one of the most promising solid electrolyte with high ionic conductivity. LTP structure is made up of two TiO_6 octahedra linked with three PO_4 tetrahedra via oxygen sharing. Lithium is present in two different types of interstitials formed by six and eight oxygen atoms, respectively. These two interstitials arranged alternatively along the conduction channels provide a three-dimensional network for Li-ion transport. In order to improve the conductivity and electrochemical properties of these materials several approaches have been developed in terms of substitution of ions such as Al, Zr, Fe, La, Mn in Ti site or by increasing Li content in the unit cell or by generating oxygen vacancies in the lattice (Kazakevicius *et al* 2008; Chen *et al* 2011). The present paper describes the effect of V^{5+} substitution in the form of $Li_{1-x}[Ti_{2-x}V_x](PO_4)_3$ on the electrochemical properties of lithium titanium phosphate material.

2. Experimental

$Li_{1-x}[Ti_{2-x}V_x](PO_4)_3$ samples with x = 0·0, 0·05, 0·1 and 0·15 are synthesized by conventional solid-state reaction method. Stoichiometric amounts of Li_2CO_3, TiO_2, $NH_4H_2PO_4$ and V_2O_5 for each composition are finely ground in an agate mortar in the presence of methanol for 6 h to obtain homogeneous mixture. The powders are then calcined at 900 °C for 4 h with a heating rate of 5 °C per min. White coloured calcined powders are pressed into pellets using PVA as binder and the pellets are sintered at 1323 K for 2 h on Pt foil.

Phase identification of sintered powders has been performed on D8 ADVANCE diffractometer of BRUKER AXS with Cu$K\alpha_1$ radiation (λ = 1·5406 Å) in the 2θ range from 10 to 70° in steps of 0·02°. Experimental densities of LTP and vanadium doped LTP pellets are measured at room temperature using standard Archimedes principle. Morphologies of fractured surfaces of pellets are examined with scanning electron microscopy on

*Author for correspondence (avrtoavr@gmail.com)

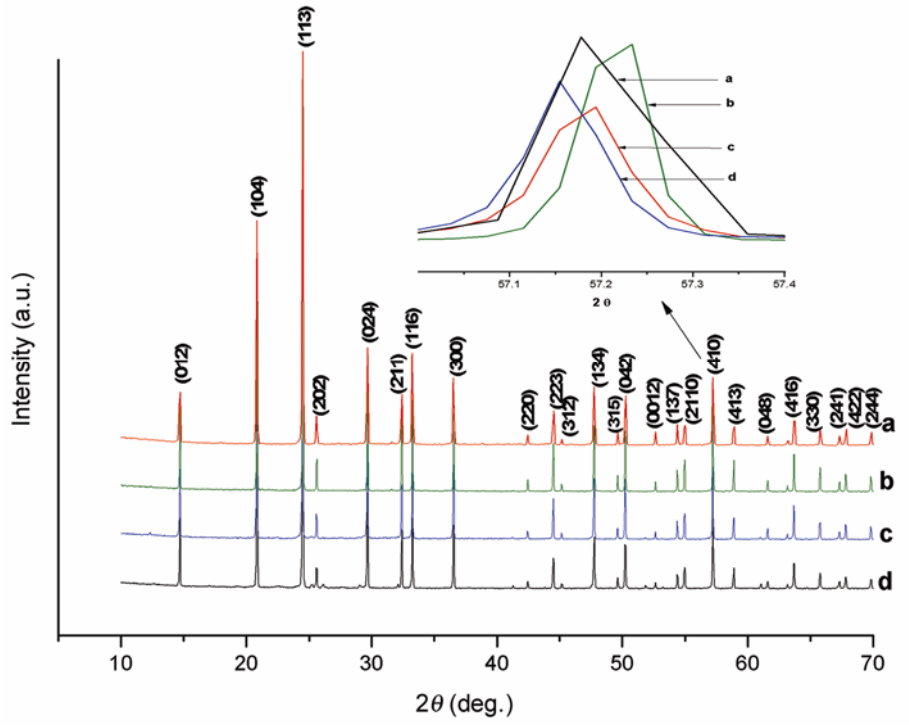

Figure 1. XRD patterns of $Li_{1-x}Ti_{2-x}V_x$ $(PO_4)_3$: (a) $x = 0{\cdot}0$, (b) $x = 0{\cdot}05$, (c) $x = 0{\cdot}1$, (d) $x = 0{\cdot}15$ sintered powders (inset, 413 peak shift).

JEOL-JSM 6610LV apparatus. Raman spectra are recorded on a RAMAN HORIBA JOBIN YVON-LABRAM-HR 800 Raman spectrometer in the frequency range of 50–1200 cm^{-1}. Ionic conductivity studies are made on pellets of 12 mm diameter and 1·5–2·5 mm thickness and the measurements are carried out on a HIOKI 3532-50 LCR HITESTER LCR meter in the frequency range from 50 Hz to 1 MHz and in the temperature range from 313 to 573 K. Electronic conductivities are noted using digital multimeter by MT 4090 LCR/ESR meter in the temperature range from 303 to 523 K. In order to understand the electrochemical window of the solid-state electrolyte LTP, a simple method of cyclic voltammetry has been carried out. The active material is coated on steel foil (cell) and then it is placed in Swagelok set up containing 1M LiPF6 dissolved in ethylene carbonate and dimethyl carbonate (1 : 1 volumetric ratio). Lithium metal is used as both counter and reference electrodes. The entire cell set up is assembled in an argon-filled glove box and tested with biologic potentiostat/galvanostat model VMP3 at a scan rate of 0·1 mV/s for three cycles between 0·5 and 3·5 V. Lithium titanium phosphate was originally studied for using it as a solid-state electrolyte and is found to react at about 2·5 V vs pure lithium in the cyclic voltammetry study (Wessells *et al* 2011).

3. Results and discussion

XRD patterns of $Li_{1-x}[Ti_{2-x}V_x](PO_4)_3$ powders sintered at 1050 °C for 2 h are shown in figure 1. XRD pattern at this temperature corresponds to phase pure compounds with rhombohedral structure and all the observed peaks could be indexed as per the JCPDS Card No. 35-0754 ($LiTi_2(PO_4)_3$). The phase formed in figure 1 is in agreement with XRD pattern for LTP indicating the formation of single phase compounds. Unit cell parameters are calculated using UNITCELL software (Unit-Cell software, 1995) and the values are shown in table 1. Lattice parameters of LTP calculated from XRD data and listed in table 1 agree with earlier reports of crystallographic data (Wang *et al* 2003; JCPDS Card No. 35-754). The lattice parameters are decreasing with increasing x value in LTP except for $x = 0{\cdot}1$. Corresponding peak shift (for 1 1 3) is observed as shown in inset of figure 1. From table 1, it is also observed that the experimental densities increased with increasing dopant concentration in LTP. Colour of vanadium doped samples after calcination/sintering is light green and as vanadium concentration increased the colour intensity also increased from light green to thick green.

Raman spectra of LTP and vanadium doped LTP samples are shown in figure 2 from which it can be seen that three intense-symmetric stretching modes appear at 967, 986, 1002 cm^{-1} along with two other antisymmetric stretching modes at 1091 and 1121 cm^{-1}. The peak at 1002 cm^{-1} is due to the symmetric stretching mode of PO_4^{3-} while the peaks at 443 and 430 cm^{-1} are due to the symmetric bending modes. Bands below 350 cm^{-1} are due to external modes and are difficult to be assigned because of mixing. Raman spectra obtained for LTP agree well

Table 1. Calculated lattice parameters and densities of LTP and vanadium doped LTP samples.

Sample name	*a* (Å)	*c* (Å)	*c*/*a*	Experimental density (g/cm^3)	Theoretical density (g/cm^3)	Relative density (%)
$LiTi_2(PO_4)_3$	8·5135	20·8705	2·4514	2·74	2·948	92·94
$Li_{0·95}Ti_{1·95}V_{0·05}(PO_4)_3$	8·5108	20·8384	2·4484	2·74	2·953	92·78
$Li_{0·90}Ti_{1·90}V_{0·10}(PO_4)_3$	8·512	20·8624	2·4509	2·76	2·947	93·65
$Li_{0·85}Ti_{1·85}V_{0·15}(PO_4)_3$	8·5101	20·8236	2·3778	2·77	2·952	93·83

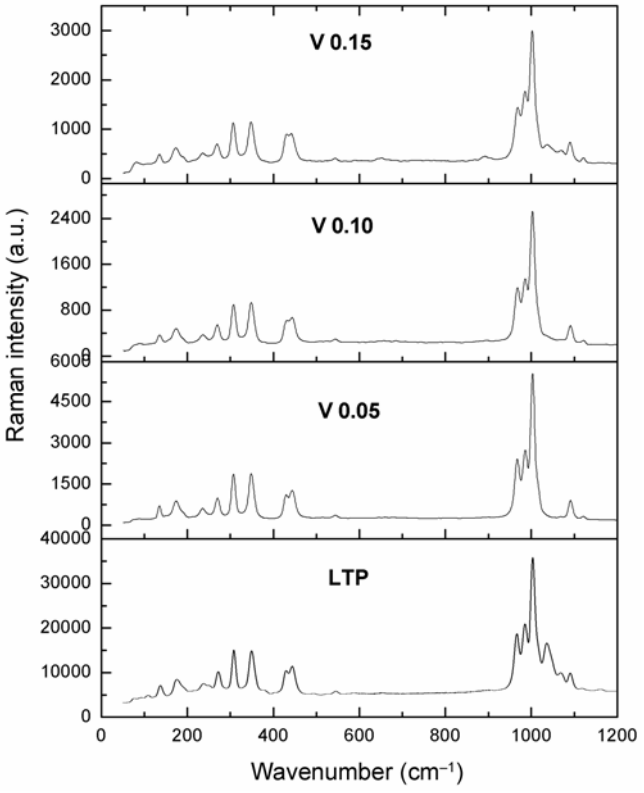

Figure 2. Raman spectra of $Li_{1-x}Ti_{2-x}V_x(PO_4)_3$ sintered powders.

with the report of Burba and Frech (2006). Vanadium substitution into LTP showed some noticeable changes on asymmetric stretching modes. All the high intense peaks got slightly shifted to lower wavenumber side with a simultaneous decrease in intensity of peaks at 1091 and 1121 cm^{-1} due to some local disordering about PO_4^{3-} ions as vanadium is inserted into the titanium site of LTP.

Figure 3 shows SEM images of fractured surfaces of pellets of LTP and vanadium doped LTP sintered at 1050 °C for 2 h. From SEM micrographs, it can be noticed that the grain size considerably increased with increase in vanadium content with certain degree of porosity. In figure 4, Cole–Cole plots for $x = 0·05$ doped LTP shows a broadened semicircle in the high frequency region at low temperature and size of the semicircle decreased with increasing temperature. The a.c. conductivity is calculated using the following equation (Sambasiva Rao *et al* 2008)

$$\sigma_{a.c.} = \varepsilon' \varepsilon_0 \omega \tan \delta, \quad (1)$$

where ε' is the relative dielectric constant, ε_0 the permittivity in vacuum, $\omega\ 2\pi f$ and $\tan \delta$ the dielectric loss. Figure 5 depicts variation of a.c. conductivity as a function of frequency at different temperatures for LTP and V-doped LTP samples. It is clear from the figure that the materials at low frequencies exhibit dispersion phenomena. Ionic conductivity increases with increase in frequency and temperature in all the doped samples. The low-frequency dispersion has been attributed to the a.c. conductivity whereas the frequency-independent plateau region in the conductivity pattern corresponds to d.c. conductivity of the material sample.

Ionic conductivities of $3·02 \times 10^{-4}$, $4·26 \times 10^{-4}$ and $5·99 \times 10^{-5}$ S/cm are observed for $x = 0·05$, 0·1 and 0·15 doped LTP samples, respectively at room temperature. But all the vanadium doped samples showed high ionic conductivity than LTP ($7·20 \times 10^{-5}$ S/cm). These results showed that the ionic conductivity is high for V ($x = 0·1$) doped LTP. Table 2 shows ionic conductivity values of LTP and vanadium doped LTP materials at different temperatures. From this table it is observed that in each composition the ionic conductivity is increasing with increasing frequency and temperature.

Figure 6 shows Arrhenius a.c. conductivity plots for $Li_{1-x}Ti_{2-x}V_x(PO_4)_3$. From the figure it is observed that the ionic conductivity continuously increased from room temperature to high temperatures, which are tabulated in table 2. The plots between $\log \sigma$ and $1000/T$ K are found to be very nearly linear obeying the Arrhenius relation. The activation energies for a.c. conductivities in different temperature regions have been obtained by measuring slope of the curves and using the relation

$$\sigma = \sigma_0 \exp[-E_a/kT], \quad (2)$$

where σ_0 is a pre-exponential factor, E_a is the activation energy, k is the Boltzmann's constant and T is the absolute temperature. The activation energy values of ionic conduction are 0·29, 0·30 and 0·31 eV for V ($x = 0·05$, 0·10 and 0·15) doped LTP samples, respectively.

The measured d.c. conductivities are $8·60 \times 10^{-9}$, $1·22 \times 10^{-8}$ and $4·30 \times 10^{-9}$ S/cm for V = 0·05, 0·1 and 0·15 doped LTP materials, respectively. Both the a.c. and

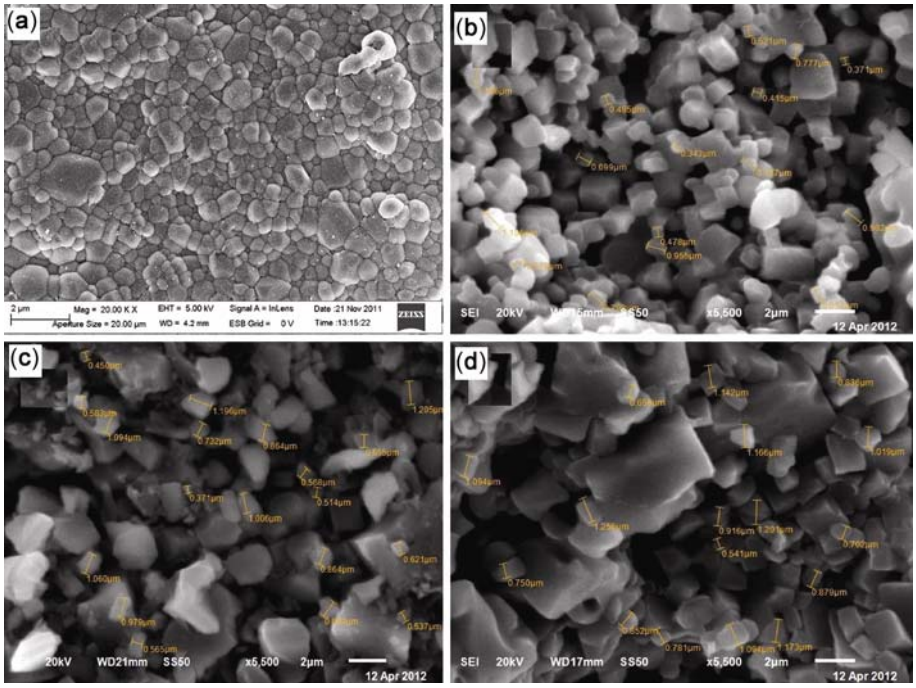

Figure 3. SEM micrographs of fractured surfaces of $Li_{1-x}Ti_{2-x}V_x(PO_4)_3$: (**a**) $x = 0{\cdot}0$, (**b**) $x = 0{\cdot}05$, (**c**) $x = 0{\cdot}1$ and (**d**) $x = 0{\cdot}15$ sintered pellets.

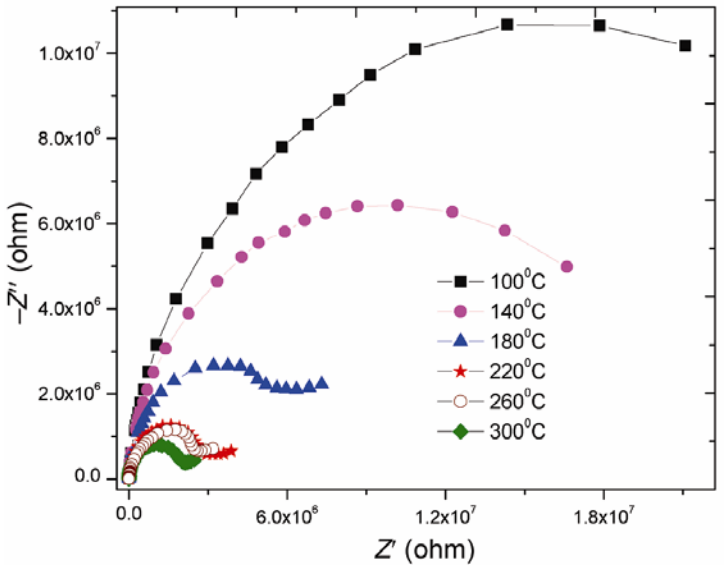

Figure 4. Cole–Cole plots of $Li_{0{\cdot}95}Ti_{1{\cdot}95}V_{0{\cdot}05}(PO_4)_3$.

Table 2. Ionic conductivities of vanadium doped LTP samples at different temperatures.

	Ionic conductivity (S/cm) at different temperatures (°C)						
Doping content	30	100	140	180	220	260	300
$x = 0$	$7{\cdot}20 \times 10^{-5}$	$7{\cdot}81 \times 10^{-5}$	$8{\cdot}27 \times 10^{-5}$	$9{\cdot}05 \times 10^{-5}$	$9{\cdot}84 \times 10^{-5}$	$1{\cdot}05 \times 10^{-4}$	$1{\cdot}13 \times 10^{-4}$
$x = 0{\cdot}05$	$3{\cdot}02 \times 10^{-4}$	$4{\cdot}95 \times 10^{-4}$	$5{\cdot}47 \times 10^{-4}$	$6{\cdot}69 \times 10^{-4}$	$7{\cdot}56 \times 10^{-4}$	$8{\cdot}28 \times 10^{-4}$	$9{\cdot}11 \times 10^{-4}$
$x = 0{\cdot}10$	$4{\cdot}26 \times 10^{-4}$	$5{\cdot}34 \times 10^{-4}$	$6{\cdot}77 \times 10^{-4}$	$7{\cdot}89 \times 10^{-4}$	$8{\cdot}97 \times 10^{-4}$	$9{\cdot}78 \times 10^{-4}$	$1{\cdot}13 \times 10^{-3}$
$x = 0{\cdot}15$	$5{\cdot}99 \times 10^{-5}$	$6{\cdot}37 \times 10^{-5}$	$8{\cdot}03 \times 10^{-5}$	$9{\cdot}22 \times 10^{-4}$	$1{\cdot}10 \times 10^{-4}$	$1{\cdot}86 \times 10^{-4}$	$2{\cdot}49 \times 10^{-4}$

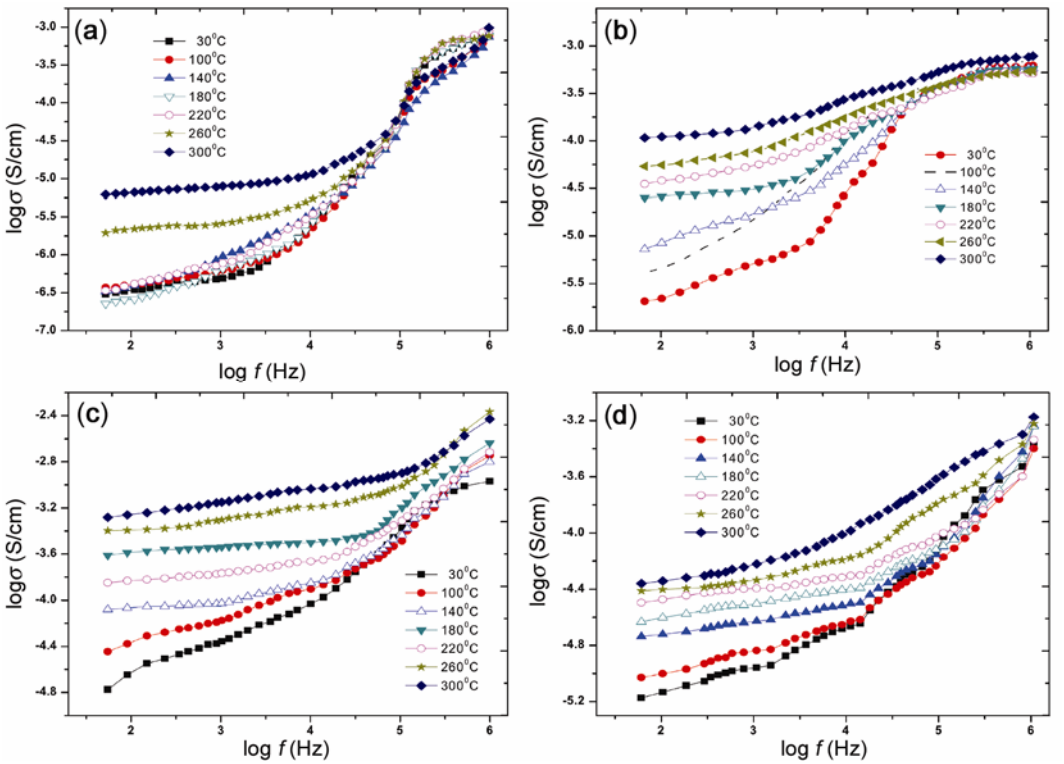

Figure 5. Frequency dependence of a.c. conductivity at different temperatures for $Li_{1-x}Ti_{2-x}V_x(PO_4)_3$: (**a**) $x = 0$, (**b**) $x = 0{\cdot}05$, (**c**) $x = 0{\cdot}1$ and (**d**) $x = 0{\cdot}15$.

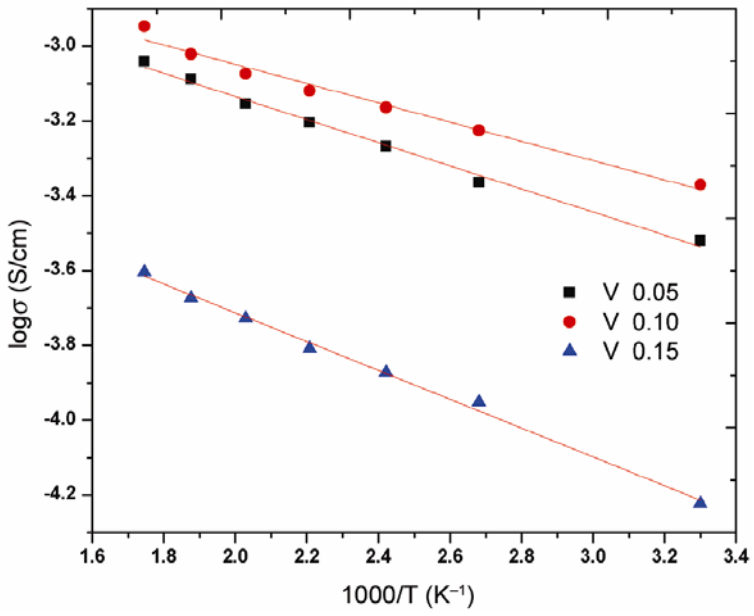

Figure 6. Variation of a.c. conductivity as a function of inverse of temperature in $Li_{1-x}Ti_{2-x}V_x(PO_4)_3$.

d.c. conductivity values are in accordance with the Jonscher's power law (Jonscher 1977). Figure 7 shows cyclic voltammogram of $Li_{0{\cdot}90}Ti_{1{\cdot}90}V_{0{\cdot}10}(PO_4)_3$ sample. Initially the reduction peaks are observed at 1·8 V, but the reduction peaks are stabilized at 2·41 V. The oxidation peaks are observed at 2·52 V. The difference between reduction and oxidation voltages is 0·13 V. The redox voltage difference of 0·13 V for vanadium dopant is less than that

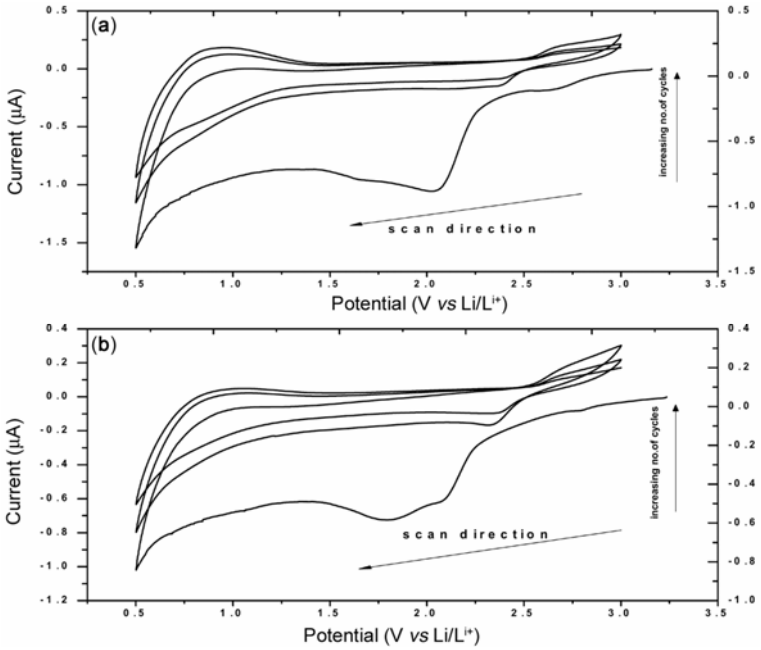

Figure 7. Cyclic voltammograms of (**a**) LTP and (**b**) $Li_{0·90}Ti_{1·90}V_{0·10}(PO_4)_3$.

observed for $LiTi_2(PO_4)_3$ which is 0·24 V. The peak intensities and electrochemical reactivity of vanadium doped samples is higher than that of LTP. This shows that the electrochemical properties of LTP are improved with vanadium doping.

4. Conclusions

Powders of different compositions corresponding to $Li_{1-x}Ti_{2-x}V_x(PO_4)_3$ (x = 0·0, 0·5, 0·1 and 0·15) have been prepared by conventional solid-state reaction method. XRD patterns of LTP heat treated at 1050 °C for 2 h showed formation of phase pure LTP of rhombohedral symmetry with space group $R\bar{3}c$ (167). Vanadium-doping in LTP led to observable shift of high intense bands to low wavenumber side along with an increase in intensity of peaks at 1091, 1121 cm^{-1} in the Raman spectra. SEM micrographs showed increased grain size of samples with increase in vanadium content. The ionic conductivity at room temperature is $4·26 \times 10^{-4}$ S/cm. A.c. conductivity studies indicated that V (x = 0·1) has resulted in high conductivity compared to 0·05 and 0·15. The measured d.c. conductivity for V (x = 0·05) is $1·22 \times 10^{-8}$ S/cm. From cyclic voltammetry results it is observed that vanadium doping concentration of x = 0·1 is good for enhancing the electrochemical properties of LTP.

Acknowledgements

Financial support in the form of UGC-SAP meritorious fellowship to one of the authors (AVR) is gratefully acknowledged.

References

Aono H, Sugimoto E, Sadaoka Y, Imanaka N and Adachi G-Y 1990 *J. Electrochem. Soc.* **137** 1023

Birke P, Salam F, Döring S and Weppner W 1999 *Solid State Ionics* **118** 149

Bruce P G, Scrosati B and Tarascon J 2008 *Angew. Chem. Int. Ed.* **47** 2930

Burba C M and Frech R 2006 *Solid State Ionics* **177** 1489

Chen Li-Juan, Zhao Yu-Jun, Jia-Yan, Luo Jia-Yan and Xia Yong-Yao 2011 *Phys. Lett.* **A375** 934

Dhivya L, Janani N, Palanivel B and Ramaswamy Murugan 2013 *AIP Advances* **3** 082115

Ellis B L, Lee K T and Nazar L F 2010 *Chem. Mater.* **22** 691

Goodenough J B and Kim Y 2010 *Chem. Mater.* **22** 587

Goodenough J B, Hong H Y P and Kafalas J A 1976 *Mater. Res. Bull.* **11** 203

Hong H Y P 1976 *Mater. Res. Bull.* **11** 173

Joint Commission on Powder Diffraction Standards (JCPDS) Card No. 35-754 (Newtown Square, PA, USA: International Centre for Diffraction Data)

Jonscher A K 1977 *Nature* **276** 673

Kasturi Rangan K and Gopalakrishnan J 1994 *J. Solid State Chem.* **109** 116

Kosova N V, Devyatkina E T, Stepanov A P and Buzlukov A L 2008 *Ionics* **14** 303

Kazakevicius E *et al* 2008 *Solid State Ionics* **179** 51

Sambasiva Rao K, Madhava Prasad D, Murali Krishna P and Joon-Hyung Lee 2008 *Physica B* **403** 2079

Unit-Cell software for cell refinement method of TJB Holland and SAT Redfern 1995

Wang G X, Bradhurst D H, Dou S X and Liu H K 2003 *J. Power Sources* **124** 231

Wessells Colin, Robert A, Huggins and Cui Yi 2011 *J. Power Sources* **196** 2884

Xia Yong-Yao and Luo Jia-Yan 2009 *J. Power Sources* **186** 224